AO4ELT7 - June 2023 - Avignon

Experimental validation of large differential piston sensing with the double-wavelength LIFT

Simone Lombardi[a], Cédric Plantet[a], Anne-Laure Cheffot[a], Marco Bonaglia[a], Alfio Puglisi[a], Chiara Selmi[a], Lorenzo Busoni[a], and Simone Esposito[a]

[a]INAF - Osservatorio Astrofisico di Arcetri, Largo Enrico Fermi 5, Firenze, Italy

ABSTRACT

Adaptive optics systems for the future Extremely Large Telescopes will have to deal with large gaps in the pupil due to the spiders and/or the segmentation of one or several mirrors. These gaps are typically larger than the expected r0 at the sensing wavelength. They can thus create significant discontinuities in the wavefront, which lead to the so-called "island effect" or "petaling": the wavefront in each segment is well corrected, but differential pistons at a multiple of the sensing wavelength appear between the segments. During the design phase of the Natural Guide star Wavefront Sensor prototype for the Giant Magellan Telescope (GMT), we have studied the Linearized Focal-plane Technique (LIFT) as a potential solution to correct the differential pistons while the adaptive optics system is running. LIFT uses a single image with a known phase offset to estimate wavefront aberrations. The reconstruction of the differential pistons from a single image is limited to the range [-lambda/2, +lambda/2], with lambda the sensing wavelength, due to the 2-pi ambiguity. However, several micrometers of capture range are needed to finely co-phase the GMT. We partially removed the ambiguity and thus increased the capture range by using two LIFT estimations at different wavelengths. At Arcetri premises we set up a test bench in order to obtain a first proof of concept for the dual-wavelength LIFT. The experimental setup includes a diffraction limited near-infrared source and a custom-made mirror with two segments. The longitudinal position of one of the halves is controlled via a motor with a precision of about 5 nm on a 10-mm range. LIFT images were taken on a defocused camera placed downstream of the segmented mirror. The dual-wavelength was achieved by alternating between two narrow-band filters. In this presentation, we show that we were able to reconstruct the differential piston either with two J-band filters or two H-band filters in the whole theoretical capture range.

Keywords: LIFT, Phase diversity, Phase retrieval, Differential piston, Giant Magellan Telescope

1. INTRODUCTION

The Adaptive Optics (AO) systems for the new generation Extremely Large Telescopes (ELT) will have to deal with a segmented pupil leading to wavefront discontinuities and thus difficulties in maintaining the phasing of the telescope [5, 1]. Indeed, with a large segmentation each segment will have its own piston aberration and the

Further author information:
S.L.: E-mail: simone.lombardi@inaf.it
C.P.: E-mail: cedric.plantet@inaf.it, Telephone: +39 055 275 2289

resulting interference causes a speckle pattern that strongly lowers the Strehl Ratio (SR) [12]. This Differential Piston (DP) between segments is poorly or not at all sensed by the most common Wavefront Sensors (WFS) in AO, the Pyramid (PyWFS) or the Shack-Hartmann (SH-WFS), in their usual configuration. Nevertheless the PyWFS is sensitive to the DP if no modulation is applied [4]. The sensitivity to DP remains at a lower level for small radii of modulation. For the fine cophasing of the Giant Magellan Telescope (GMT), the modulation radius of 2 λ/D will provide both the classical AO wavefront sensing and a measurement of the DP [2]. Still, the uncertainty of $n \cdot 2\pi$ in the phase remains, and the range to sense the piston is limited to $-\lambda/2, +\lambda/2$. This limitation can result in segment ejections at multiples of the sensing wavelength [8]. Therefore a dedicated sensor with a wider range is needed to keep the telescope phased during the AO loop. This sensor could be placed as a second channel which runs in parallel with the main (PyWFS) one. In the case of the GMT, the correction of the DP will be done using the Holographic Dispersed Fringe Sensor (HDFS) [6]. The backup solution for this second channel is the LInearized Focal plane Technique (LIFT) [7], adapted to this application. As the feasibility of the project has already been numerically demonstrated [11], the main point of our work was to implement a lab prototype to prove that the system is indeed capable of measuring the DP between two segments in all of the GMT's AO dynamic range. In this paper we describe how LIFT can be used to measure the DP and the procedure to extend its range beyond $-\lambda/2, +\lambda/2$. We then describe our experimental setup and how we performed the measurements. Finally we conclude with a very brief discussion of the system main weaknesses and the next steps of this work.

2. MEASUREMENT PRINCIPLE

2.1 Single wavelength algorithm

The measurements of the Differential Piston (DP) in the canonical range of $[-\lambda/2, +\lambda/2]$ in wavefront is performed as an application of the Linearized Focal Plane Technique (LIFT) algorithm in the monochromatic approximation, which is hereafter called the Single Wavelength Algorithm (SL) [7]. The LIFT algorithm is able to retrieve the coefficients of wavefront modes from a single image, and it has already been tested on sky on GeMS [10]. From the hardware point of view it just needs a camera on the system focal plane. To solve the problem of the phase indetermination a known aberration needs to be added in the system. To use LIFT as a DP WFS we can specify a set of DP modes to directly take into account the WF steps between the segments (see Fig.1). The main problem in this concept is that there can be some cross-talk between the DP modes and other modes in the residuals of the AO correction, therefore the existence of a unique solution is not necessarily true. In the case of GMT, a simulation study demonstrated that it is possible to retrieve the six DP terms at the same time if a strong enough defocus aberration is used.

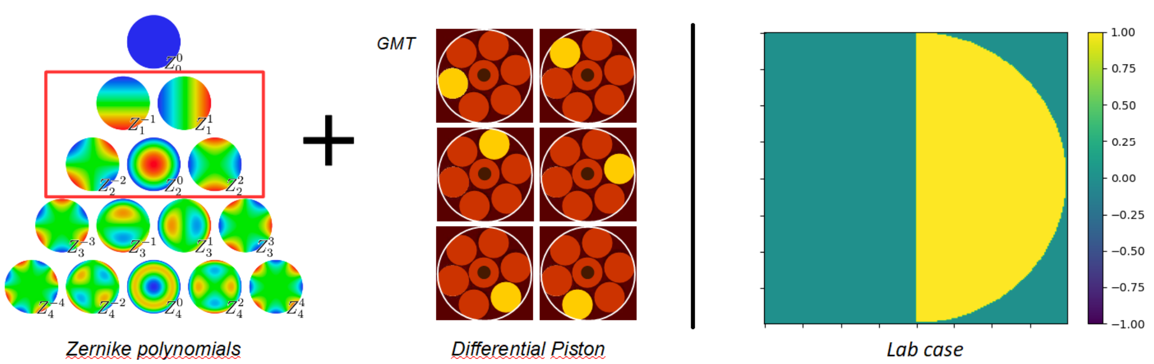

Figure 1. On the left we show the normal modes (Zernike ones) used to estimate the residual aberration of the system and the DP modes used to perform the numerical study on GMT. On the right it's shown the DP mode used in the lab experimental case.

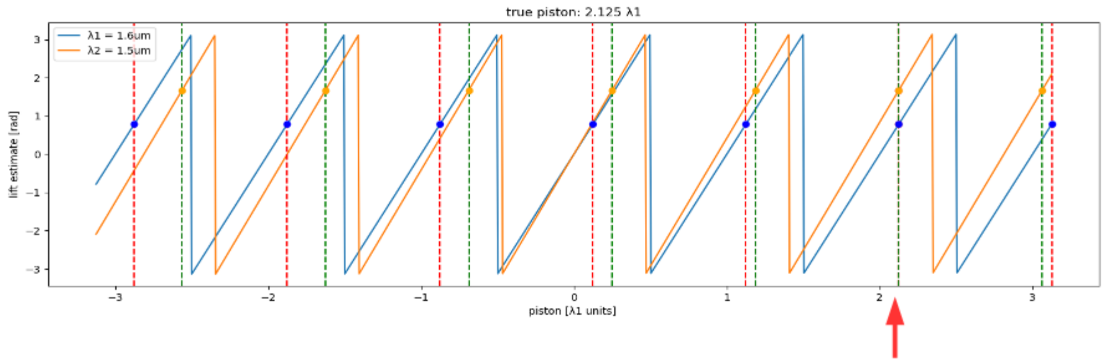

Figure 2. Diagram of the DW algorithm basic mechanism. As we move further and further from the coherence position in which the red and blue curve overlap, the phase separation between the two keeps growing and there exists only one point (the red arrow) in the range of $\pm\Lambda/2$ such that the two estimation of the DP are the same, with Λ the synthetic wavelength.

2.2 Double Wavelength algorithm

Besides the cross-talk problems between classical modes and DPs, the main issue with the application on GMT is the range of the measurement. That is of course because the effects of the DPs on the intensity pattern are periodic and therefore any monochromatic WFS will present the well-known 2π uncertainty. The common solution to that is the introduction of a second wavelength (WL) and the measurement of the DP also for this new WL. See fig. 2. This procedure was first suggested for the application of the Pyramid Wavefront Sensor (PyWS) to the estimation of DPs [4]. In short what we want to do is to retrieve the right solution from two different ones, with their own $n \cdot 2\pi$ uncertainty. For each lambda we calculate the DP and look for all the solutions within the desired range. We then compute the separation between all the couples of points and retrieve the true DP as the position with the minimum difference between the two lambdas. We have to highlight how the maximum range cannot exceed the beat WL (Λ) between the two original waves, that is the reason for which we need them to be as close as possible 1.

$$\Lambda = \frac{\lambda_1 \cdot \lambda_2}{|\lambda_1 - \lambda_2|} \tag{1}$$

Beyond the limit of the beat WL the solution gets periodic again, but as long as we apply the Double Wavelength Algorithm (DW) for the DP reconstruction the system can be considered as a SW one with an equivalent WL of Λ. In a previous study the most promising bands for the GMT application were H (1600nm, 1500nm) and J (1250nm, 1150nm) [9], therefore those were also the ones we focused on .

3. EXPERIMENTAL SETUP

3.1 Optical bench

The setup used to take the measurements is shown in Fig. 3 on the left. The source was a point like source from a monochromatic optical fiber (core diameter 5 um) from a IR camera ($<\lambda>= 1400nm$, $BW = 500nm$). The beam then is collimated by a parabola (f= 15 cm) and sent to the segmented mirror. This piece consisted in a two-segments circular mirror, both able to translate along the Optical Axis and with tip and tilt regulations. The segmented mirror was responsible for the introduction of the step-like phase discontinuity in the collimated beam. The two segments were also at a known distance (gap) of 1.7mm c.a. from each other. Using a beamsplitter (BS1) the aberrated beam is sent through a pinhole (the pupil) and is focalized on the camera by the lens. Lastly the filter wheel was used to select the band. Since the sensitivity of the process is dependent on the F#, we chose pinhole (diameter D) to obtain the ratio $f/D = 30$ with f the focal length of the lens. The IR camera was the last relevant component of the optical train and could be moved along the optical axe to introduce the defocus aberration. Finally the optical design included a secondary path used for the alignment of the segments' tip and tilt (TT), which proved to be of the utmost importance. This makes the part of the AO's TT correction on each segment. As shown in the Fig. 3 a reference common mirror was used to implement a Michelson Interferometer for each segment. They were considered aligned when the size of the fringes was comparable with the diameter of the beam. We estimated the precision of the segment tip-tilt alignment at about 2.5e-5 rad which proved to be sufficient for a complete reconstruction. To operate this portion of the bench a 650nm laser was used (Fig.3 on the right).

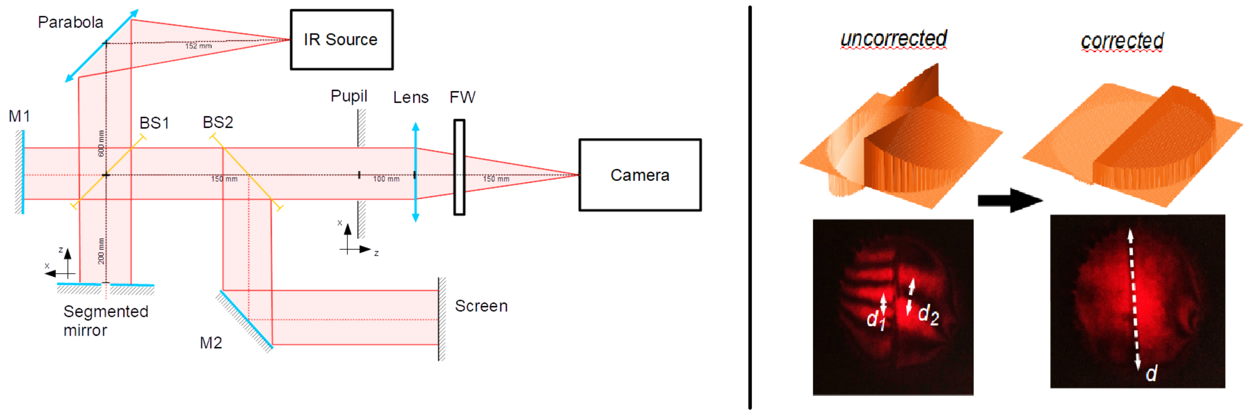

Figure 3. Left: schematic of the optical bench with all of its components. Right: example of the discontinuous fringe pattern that appears on the screen after M2 before and after the tip ant tilt alignment of the two portions of the segmented mirror. When the spacing of the fringes (d_1 and d_2) for both the halves of the mirror is comparable with the diameter of the beam (d) the maximum precision is achieved.

3.2 Data acquisition

Before the acquisition of the data we needed to make sure that the segments were within $\Lambda/2$ from each other to prevent the $n \cdot 2\pi$ ambiguity in the DW algorithm. We used a procedure close to the one already tested for the Keck telescope [3], performing a scan (we moved one of the segments in respect to the other) along the optical axe around the in-phase position of the segments. The segments are considered to be phased when the intensity of the fringe pattern on the focal plane is at its maximum. To obtain the best possible result, we performed a first narrow band scan (1600 nm, 50 nm BW) followed by a broad band scan ($< 1400 > nm$,500 nm BW) with a final precision of $\pm 2um$. Both were needed as the precision of the narrow band was to low, and the range of the broad band was too short. See fig. 4. The final data acquisition was again a scan around the in-phase position but moving the camera to the off-focus position (15 mm). For each position in the scan, the image for both the WLs were saved to perform the DP reconstruction offline.

4. FINAL RESULTS

4.1 DP reconstruction

We were able to perform the reconstruction of the DP for both the H and J WLs over the full range of the DW algorithm (fig. 5). The desired result was for a precision of 100 nm at most as below such a treshold GMT's main AO channel is able to perform the fine phasing of the mirror since the residual DP is within its capture range. With this in mind we measured the errors of the single estimations and those never exceeded $\lambda/10$, while the errors for the points closer to the in-phase position (meaning withing 0.5 um) were inferior to $\lambda/100$, well within our requirements. In fig. 5 we can also appreciate as the superior coherence length of the J band grants a better analysis on a much larger range than the H band.

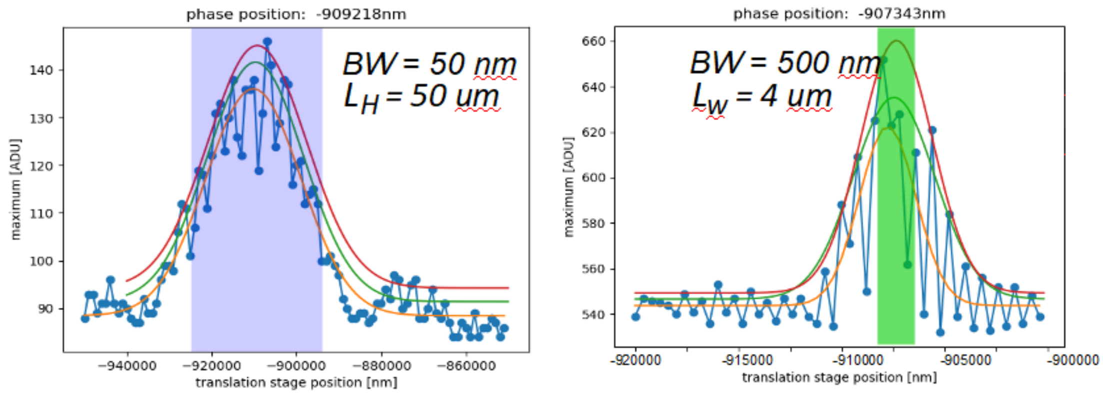

Figure 4. Example of the narrow band and the broad band scan. The colored section is the coherence length for the corresponding bandwidth. We can appreciate the superior precision of the broad band scan and the much larger range of the narrow band.

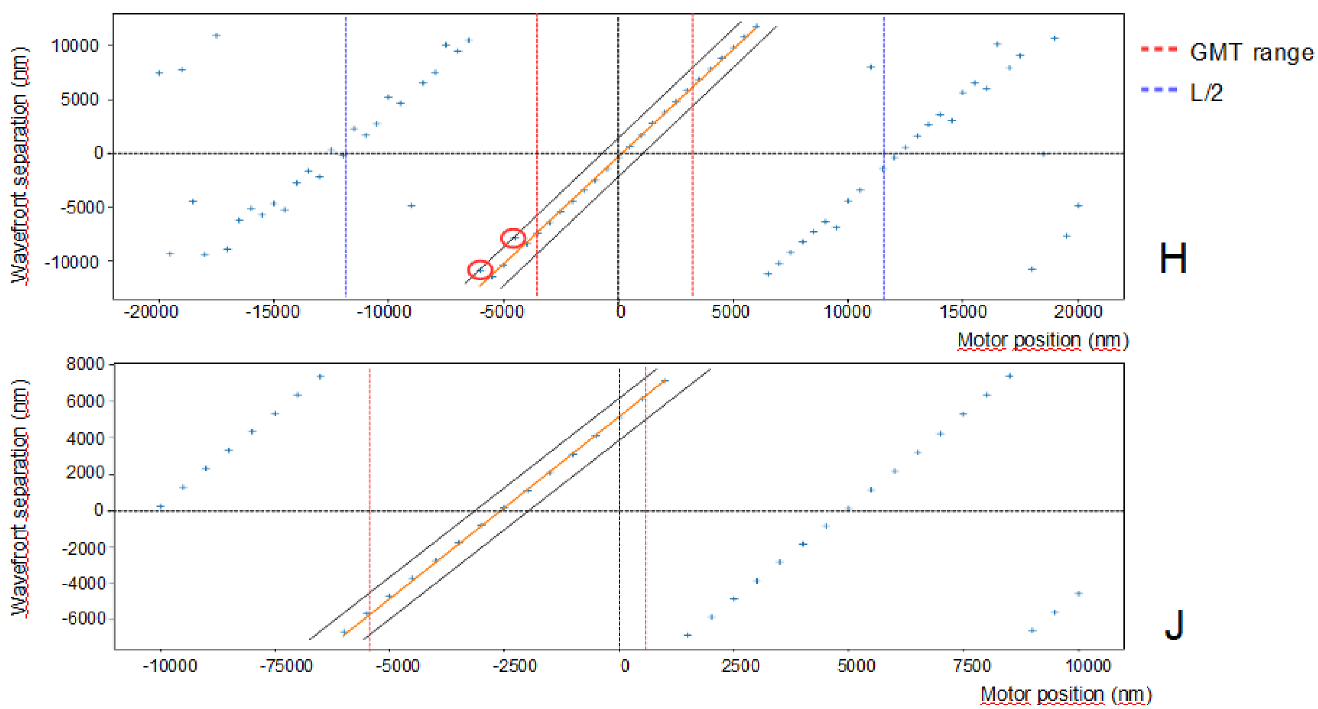

Figure 5. Final reconstruction for both the H (top) and J band (bottom). Each blue point is a value of the DP. In the H band the red circles mark the only two points which present an error of 2π. The dotted red lines marks the requirements of GMT's range while the blue ones are the limits of the coherence length. The black lines parallels to the perfect solution are the 2π interval.

4.2 Discussion

Even thought LIFT provided very good results it requires some attention in some more technical aspects. We did not find any real problem with the cross talk between the normal modes and the ones describing the DP 2.1, instead we found out that whatever effect produces a similar intensity pattern to that of the DP can reduce the precision of the measurement. In particular the system is quite sensitive to the differential flux between the segments, to the point that a small (up to 10%) difference in the flux can lead to a wrong estimation of the DP (in the order of hundreds of nanometers) Fig. 6. There can be several reason to this difference in flux, and in our case we found out that, due to the apodization of the beam from the optical fiber, the alignment of the pupil and the gap (they were separated on our test bench Fig. 3) with the center of the beam is of the outmost importance. Unfortunately we weren't able to find any way to reduce such an error other than to directly improve the conditions on the optical bench.

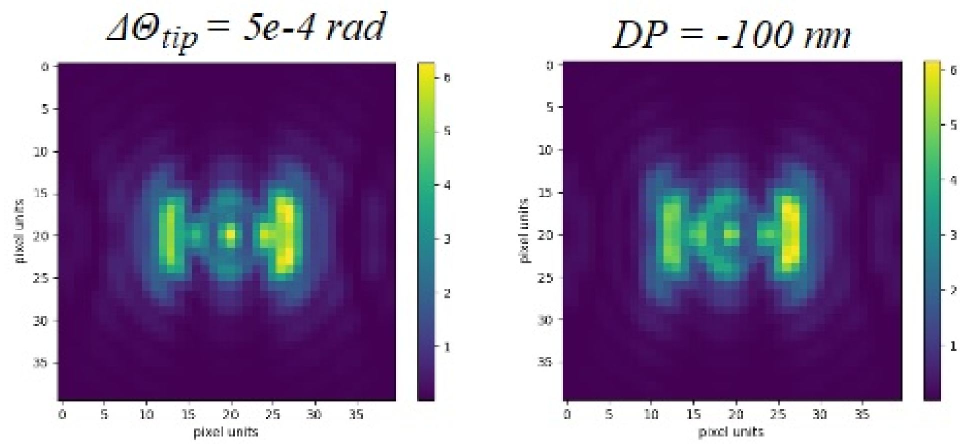

Figure 6. The two images show how a difference in flux produces an effect which is almost the same of a small DP. On the left there is the pattern produced with a tip aberration which reflects on a asymmetric projection of the gap on the pupil plane and zero DP, while on the right the DP is the only aberration of the beam. In both cases the right lobe appears a lot brighter without any change in the shape of the PSF.

5. CONCLUSIONS

We consider proved the feasibility of the DP estimation using the LIFT algorithm together with the DW one in the simple and controlled case of two identical segments composing a circular mirror, separated by a gap of known width and with no turbulence residuals disturbing the analysis. At the same time we realized the importance of the differential flux between the pupil segments which needs to be as close as possible to zero and proved to be LIFT main issue. In the future we intend to test the performance of the algorithm when AO residuals are present. We also plan to perform a proper study of the errors in the SW estimation and their dependence on the DP amplitude, as well as their propagation in the DW algorithm. The final goal would be to test LIFT in a GMT-like configuration, where the algorithm would have to deal with several DPs within a same pupil.

References

[1] Guido Agapito et al. "MAORY/MORFEO and LIFT: can the low order wavefront sensors become phasing sensors?" In: *Adaptive Optics Systems VIII*. Ed. by Laura Schreiber, Dirk Schmidt, and Elise Vernet. Vol. 12185. International Society for Optics and Photonics. SPIE, 2022, p. 1218556. DOI: 10.1117/12.2629352. URL: https://doi.org/10.1117/12.2629352.

[2] Pinna E. Agapito G. Quirós-Pacheco F. Antichi J. Carbonaro L. et al. *Design and numerical simulations of the GMT Natural Guide star WFS*. SPIE Astronomical Telescopes + Instrumentation, 2014, Montréal, Quebec, Canada.

[3] Gary Chanan and Mitchell Troy et al. *Phasing the mirror segments of the Keck telescopes: the broadband phasing algorithm*. 1998 Optical Society of America.

[4] S. Esposito and N. Devaney. *Segmented telescopes co-phasing using Pyramid Sensor*. NASA Astrophysics Data System, January 2002.

[5] James Fanson et al. "Overview and status of the Giant Magellan Telescope project". In: *Ground-based and Airborne Telescopes IX* (2022). DOI: 10.1117/12.2631694. URL: https://giantmagellan.org/wp-content/uploads/2023/04/SPIE22.pdf.

[6] Sebastiaan Y. Haffert et al. "Phasing the Giant Magellan Telescope with the holographic dispersed fringe sensor". In: *Journal of Astronomical Telescopes, Instruments, and Systems* 8.2 (2022), pp. 1–21. DOI: 10.1117/1.JATIS.8.2.021513. URL: https://doi.org/10.1117/1.JATIS.8.2.021513.

[7] Serge Meimon, Thierry Fusco, and Laurent M. Mugnier. *LIFT: a focal-plane wavefront sensor for real-time low-order sensing on faint sources.* OCIS codes: 010.1080, 010.7350: Optical Society of America, 2010.

[8] E. Pinna et al. "Design and numerical simulations of the GMT Natural Guide star WFS". In: *Adaptive Optics Systems IV*. Ed. by Enrico Marchetti, Laird M. Close, and Jean-Pierre Véran. Vol. 9148. International Society for Optics and Photonics. SPIE, 2014, pp. 898–912. DOI: 10.1117/12.2057059. URL: https://doi.org/10.1117/12.2057059.

[9] Cedric Plantet and Anne Laure Cheffot et al. *NGWS-P: the Natural Guide star Wavefront Sensor Prototype of GMT single conjugate AO system NGAO.* NGWS$_{PS}PIE$, 2022.

[10] Cedric Plantet et al. *On-sky validation of LIFT on GeMS.* May 2013, Third AO4ELT Conference - Adaptive Optics for Extremely Large Telescopes.

[11] Cédric Plantet et al. "NGWS-P: the natural guide star wavefront sensor prototype of GMT single conjugate AO system NGAO". In: *Adaptive Optics Systems VIII*. Ed. by Laura Schreiber, Dirk Schmidt, and Elise Vernet. Vol. 12185. International Society for Optics and Photonics. SPIE, 2022, 121854H. DOI: 10.1117/12.2630864. URL: https://doi.org/10.1117/12.2630864.

[12] Natalia Yaitskova, Kjetil Dohlen, and Philippe Dierickxarl. *Analytical study of diffraction effects in extremely large segmented telescopes.* 2003 Optical Society of America.